Synthesis of Thermally Stable Organosilicate for Exfoliated Poly(ethylene terephthalate) Nanocomposite with Superior Tensile Properties

Ki Hong Kim, Keon Hyong Kim, June Huh, and Won Ho Jo*

Hyperstructured Organic Materials Research Center and School of Materials Science and Engineering, Seoul National University, Seoul 151-742, Korea

Abstracts: A poly(ethylene terephthalate) (PET)/organosilicate nanocomposite, with enhanced mechanical properties, has been prepared using the melt intercalation method. For this purpose, a new organic modifier has been synthesized for the preparation of organosilicate, which is thermally stable and compatible with PET. The use of the new organosilicate yielded almost exfoliated PET nanocomposite; whereas, the PET nanocomposites prepared by use of commercial organoclays (Cloisite 15A and 30B) show only an intercalated morphology. Particularly, the use of the new organosilicate showed an enhanced tensile modulus, and without sacrifice of the tensile strength and elongation on breaking, while the use of commercial organoclays only exhibit a trade-off between those mechanical properties.

Keywords: poly(ethylene terephthalate), nanocomposite, melt intercalation, organic modifier, mechanical properties.

Introduction

Since the Toyota research group developed the nylon-6/clay nanocomposite,[1-3] the polymer/clay nanocomposite has been widely used for developing new polymeric composites that may provide many excellent physical properties. This substantial attention on polymer/clay nanocomposites is attributed to the fact that they show significant improvement in moduli,[4-7] strength,[8] thermal resistance,[8] gas barrier property,[9-12] and fire retardance[13-16] as compared to virgin polymers or conventional microcomposite counterparts containing an equivalent volume fraction of inorganic filler. Two main approaches can be used to prepare polymer/clay nanocomposites: melt intercalation[17-19] and in-situ polymerization.[20-23] In the process of melt intercalation considered as commercially more viable approach, the layered silicate, which is the basic building unit of natural or synthetic clay, is directly melt-mixed with a molten polymer. If the surface-modified silicates are compatible with the matrix polymer, the polymer chains in melt may diffuse into the galleries between the silicate layers, leading to intercalated, exfoliated or a coexistence of these two morphologies.

Poly(ethylene terephthalate) (PET) is sharing a large volume of market and has been used for fibers, bottles, films, and engineering plastics for many years due to its low cost and high performance.[24] This wide range of applications of PET can be even more extended by incorporation of clay into PET matrix, because well-dispersed silicate layers may enhance various physical properties of PET such as gas barrier property and fire retard. For this reason, several workers have attempted to disperse and/or exfoliate silicate layers in PET matrix via the melt intercalation method.[25-27] In those studies, PET was directly melt-mixed with a commercial organoclay containing quaternary ammonium cation as an organic modifier. However, those PET nanocomposites showed only an intercalated morphology, which was mainly attributed to the fact that the organic modifier residing in commercial organoclays was not compatible with PET. Moreover, the commercial organoclays are thermally unstable at the processing temperature of PET (~280 °C) probably because the quaternary ammonium cation bound to the silicate surface is thermally unstable. It has been reported that the thermal decomposition temperature of commercial organoclays is below 200 °C.[28] Actually, in recent years, it has been demonstrated that the thermal stability of organically modified silicates (organosilicates) plays a critical role in preparation and processing of polymer/clay nanocomposite,[28,29] because the thermal decomposition of the organic modifier alters the interface between the organosilicates and polymer matrix. Therefore, it is very likely that one key parameter yielding an exfoliated PET/clay nanocomposite using the melt intercalation method is to improve the thermal stability of organosilicates. In this context, Davis *et al.*[30] prepared PET nanocomposites by melt-mixing of PET and organosilicates modified with 1,2-dimethyl-3-*N*-alkyl imidazolium salt. Although they claimed that the organosilicates were

*Corresponding Author. E-mail: whjpoly@snu.ac.kr

thermally very stable and that the prepared PET nanocomposites showed a high level of dispersion and exfoliation of silicates in PET matrix, they did not report mechanical properties of their PET nanocomposites. Another important point to be considered for exfoliated PET nanocomposite is that the organosilicates must also be compatible with the PET matrix; otherwise the organosilicates will not be dispersed effectively in the PET matrix during the melt-mixing process and thus a significant improvement in mechanical properties of the PET nanocomposite will not be expected.

In this paper, we report the preparation of new organosilicate, which is thermally stable and also compatible with PET for preparation of PET/organosilicate nanocomposite. For this purpose, a new organic modifier satisfying the following two conditions is synthesized: (1) it has a functional group compatible with PET and (2) it also has a cationic group which is thermally stable at the melt-mixing temperature of PET and organosilicate (~280°C). To satisfy the conditions (1) and (2), we synthesize an organic modifier with a hydroxyl group as the functional group and an imidazolium cation as the cationic group. Then, PET is melt-mixed with the new organosilicate modified with imidazolium cation to prepare exfoliated PET nanocomposite. For comparison, PET nanocomposites are also prepared using commercial organoclays such as 15A and 30B, and then morphological structure and mechanical properties of new PET nanocomposite are compared to those of nanocomposites prepared from commercial organoclays.

Experimental

Materials. 1,2-Epoxy-3-phenoxypropane, 2-bromoethanol, 1,2-dimethylimidazole, and magnesium perchlorate were purchased from Aldrich Chemical Co. and used as received. Acetonitrile used as solvent was also purchased from Aldrich Chemical Co. and dried by distillation over CaH_2 and molecular sieve 4A. Na-montmorillonite (Na-MMT) with cation exchange capacity (CEC) of 92 meq/100 g was supplied from Southern Clay Products (Gonzales, Texas) and used as received. Cloisite 15A and 30B, which were montmorillonites modified with dimethyl dihydrogenated tallow alkyl ammonium and methyl tallow bis(2-hydroxyethyl) alkyl ammonium, respectively, were also obtained from Southern Clay Products and used after drying at 100°C under vacuum for 12 h. PET pellets were obtained from Hyosung Co. and dried at 120°C under vacuum prior to use.

Synthesis of 1-(2-Bromo-ethoxy)-3-phenoxy propan-2-ol (1). The overall synthetic route to 1-[2-(2-hydroxy-3-phenoxy-propoxy)-ethyl]-2.3-dimethyl-3H-imidazolium bromide (DMIBr) was represented in Figure 1. The precursor for synthesis of DMIBr, 1-(2-bromo-ethoxy)-3-phenoxy propan-2-ol (1), was synthesized as follows: A solution of the 1,2-epoxy-3-phenoxypropane (18 mL, 0.133 mol) in acetonitrile was treated with anhydrous magnesium perchlorate (30 g, 0.133
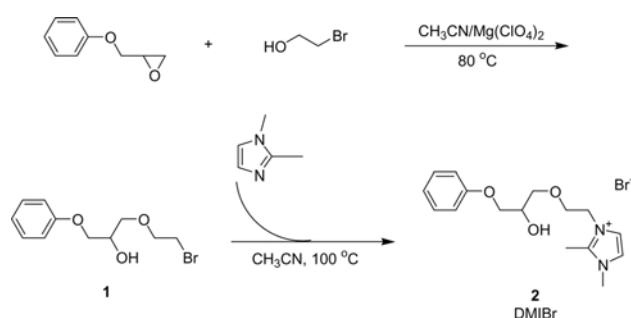

Figure 1. The overall synthetic route to DMIBr.

mol), and then the solution of mixture was stirred until the solution became homogeneous. The resulting solution was reacted with 2-bromoethanol (19 mL, 0.266 mol) at 80°C under stirring for 24 h under nitrogen atmosphere. The reaction mixture was diluted with H_2O and then extracted with diethyl ether. The crude product in diethyl ether layer was condensed by evaporation of diethyl ether, and the residue was purified by a silica column chromatography using a mixed solvent of ethyl acetate and *n*-hexane (50:50/v:v) as an eluting solvent. The yield was 5.1 g (0.019 mol, 14%). ^{1}H NMR (CDCl$_3$): δ=7.32~6.91 (m, 5H, Ar-O-), 4.21~4.15 (m, 1H, -CH$_2$-CH(OH)-CH$_2$-), 4.07~4.04 (d, 2H, -CH(OH)-CH_2-O-), 3.86~3.82 (t, 2H, -O-CH_2-CH$_2$-), 3.75~3.64 (m, 2H, -O-CH_2-CH(OH)-), 3.51~3.47 (t, 2H, -CH$_2$-CH_2-Br). C$_{11}$H$_{15}$BrO$_3$ (275.14): Calcd. C 48 .02, H 5.50, O 17.44; found C 48.22, H 5.57, O 17.27.

Synthesis of DMIBr (2). A solution of **1** (0.8 g, 0.003 mol) in acetonitrile was reacted with 1,2-dimethylimidazole (1.0 g, 0.01 mol) at 100°C for 7 days under nitrogen atmosphere. The product was solidified in the reaction mixture during the reaction. The solid product was redissolved in DMSO and precipitated in ethyl acetate. The precipitate as the product (**2**) was collected as brown solid by filtration and subsequent washing with ethyl acetate, and then dried at 80°C under vacuum. The yield was 0.8 g (0.0022 mol, 73%). ^{1}H NMR (DMSO-d$_6$): δ=7.69~7.65 (d, 1H, -N$^+$-CH=CH-), 7.63~7.59 (d, 1H, -CH=CH-N(CH$_3$)-), 7.35~6.87 (m, 5H, Ar-O-), 4.34 ~4.30 (t, 2H, -CH$_2$-CH_2-N$^+$-), 3.93~3.80 (m, 1H, -CH$_2$-CH(OH)-CH$_2$-), 3.84~3.83 (d, 2H, -CH(OH)-CH_2-O-) 3.76~3.73 (t, 2H, -O-CH_2-CH$_2$-), 3.71 (s, 3H, =CH-N(CH_3)-C(CH$_3$)=), 3.53~3.43 (m, 2H, -O-CH_2-CH(OH)-), 2.57 (s, 3H, -N(CH$_3$)-C(CH_3)=N$^+$-). C$_{16}$H$_{23}$N$_2$O$_3$ (371.27): Calcd. C 51.76, H 6.24, O 12.93, N 7.55; found C 51.34, H 6.24, O 12.82, N 7.66.

Preparation of Organosilicate and PET/Organosilicate Nanocomposites. The new organosilicate (DMIBrC) was prepared by exchanging Na$^+$ ion in Na-MMT with DMIBr. The DMIBr was dissolved in a mixed solvent of DMSO:H$_2$O (50:50/v:v) and stirred at 70°C. 1 g of Na-MMT was suspended in 100 mL of H_2O and then the suspended solution was added to the DMIBr/DMSO/H$_2$O solution. The mixture was vigorously stirred at 70°C for 12 h. When the product

was precipitated, the precipitate was collected by filtration and washed subsequently with DMSO, H_2O and methanol until an $AgNO_3$ test indicated the absence of bromide ion. The filter cake as the reaction product (DMIBrC) was dried at 80 °C under vacuum for 24 h.

PET/DMIBrC nanocomposite was prepared by the melt-mixing of PET with the DMIBrC in a ratio of 97/3 by weight using a mini-max molder at 280 °C for 10 min. Before melt-mixing, PET was thoroughly dried at 120 °C under vacuum for 24 h. For comparison, PET/30B and PET/15A nanocomposites were also prepared under the same mixing condition.

Measurements. The change in the basal spacing of organoclays and PET nanocomposite was measured using an X-ray diffractometer (XRD) (MAC Science, MXP 18A-HF). Ni-filtered $CuK\alpha(\lambda=1.54 \text{ Å})$ radiation, generated at a voltage of 40 kV and current of 30 mA, was used as an X-ray source. The diffraction angle was scanned from 1.5 to 10° at a rate of 2°/min. The morphological structure of PET nanocomposites was also characterized using a Philips-CM20 transmission electron microscopy (TEM), operated at an accelerating voltage of 200 kV. Sections of 70 nm in thickness were ultramicrotomed with a diamond knife and then mounted on 200 mesh copper grids. Since silicate layers had higher electron density than PET, they appeared dark in bright-field TEM image.

To investigate the thermal stability of DMIBrC, thermogravimetric analysis (TGA) was conducted on a TA instrument 2050 under nitrogen atmosphere. The sample was heated from room temperature to 800 °C at a rate of 10 °C/min.

Tensile properties of the neat PET and PET nanocomposites were measured using a universal testing machine (UTM). Rectangular-shape tensile test specimens of 1 mm in thickness and 2.5 mm in width were prepared by compression molding according to the specification ASTM D-638 type III. The tensile properties were measured at room temperature at a constant cross-head speed of 2.5 mm/min. At least five specimens were tested for each sample and the tensile properties are reported on average.

Results and Discussion

Thermal Stability. As mentioned in the introduction, the thermal stability of organosilicates plays a critical role in preparing exfoliated PET/clay nanocomposites, considering that the processing temperature of PET is high (~280 °C). Hence, the thermal stability of DMIBrC is examined by TGA measurement before they are dispersed in PET matrix. For comparison, TGA measurement for 15A and 30B is also carried out at the same condition. The weight loss curves of organosilicates are shown in Figure 2(a), and their thermal stabilities are summarized in Table I. As can be seen in Table I, the onset temperature of decomposition of DMIBrC
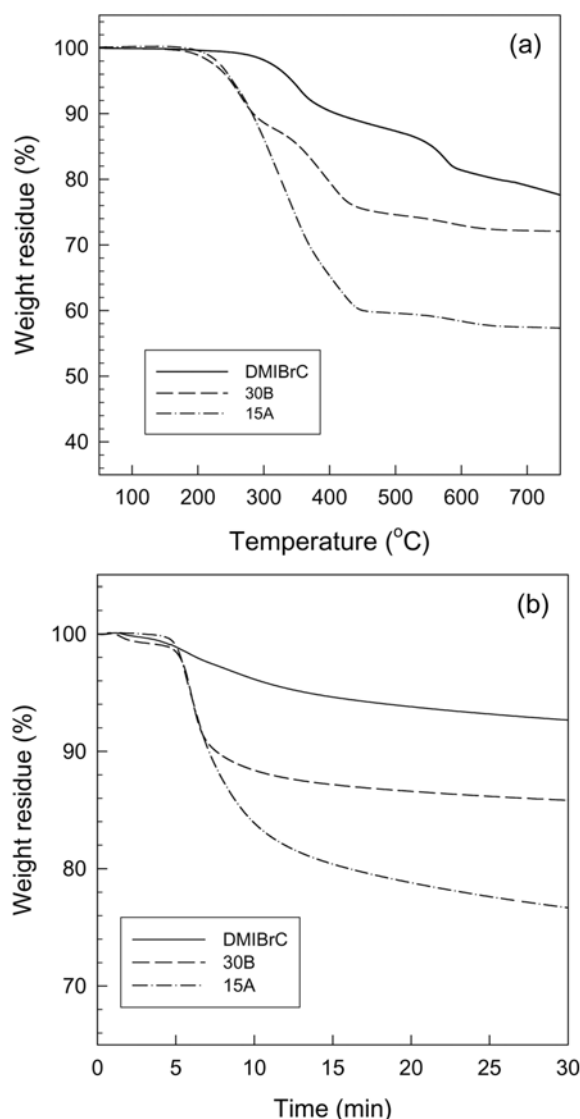

Figure 2. (a) TGA curves of organosilicates and (b) weight loss curves of organosilicates from the isothermal TGA measurement. The isothermal TGA measurement is carried out at 280 °C under nitrogen atmosphere.

(255 °C) is 60 °C higher than that of 15A and 30B (196 °C and 174 °C, respectively). Moreover, the weight loss of DMIBrC is only 1% at the melt-mixing temperature of PET (~280 °C), whereas the weight loss of 15A and 30B (~10%) is larger than that of DMIBrC at the same temperature (280 °C), as seen in Figure 2(a) and Table I. The isothermal TGA measurement is carried out at 280 °C to confirm the enhanced thermal stability of DMIBrC at the processing temperature of PET. Figure 2(b) compares the weight losses of the organosilicates at 280 °C as a function of time. After 10 min, corresponding to the melt-mixing time for PET nanocomposites, the weight loss of DMIBrC (~4%) is very small compared to that of 15A and 30B (~17 and ~12%, respec-

Table I. Characteristics of Organosilicates Measured from TGA and XRD

Organosilicates	The Onset Temperature (°C)[a]	The Weight Loss at 280°C (%)	The Weight Loss after 10 min (%)[b]	Basal Spacing (nm)
15A	196	10	17	3.5
30B	174	10	12	1.8
DMIBrC	255	1	4	1.6

[a] The onset temperature is determined from the derivative curves of TGA data. [b] The weight loss after 10 min is determined from the isothermal TGA data at 280°C.

tively) (see also Table I). From these TGA results, it is concluded that DMIBrC is thermally stable during melt-mixing with PET.

Morphological Structure. The layered structure of DMIBrC is analyzed by XRD to examine whether or not the organic modifier (DMIBr) is successfully intercalated between the silicate layers of Na-MMT. The XRD patterns (see Figure 3(a)) clearly show that the (001) reflection peak ($2\theta = 5.5°$) for DMIBrC shifts to lower angle compared to that of Na-MMT ($2\theta = 7.3°$). This shift in the (001) reflection peak to lower angle is a direct evidence for the fact that the basal spacing of layered silicates is increased by intercalation of DMIBr into silicate layers of Na-MMT. Table I summarizes the basal spacing for DMIBrC synthesized in this study along with the basal spacings of commercial organoclays.

The morphological structure of the PET nanocomposites is investigated by XRD and TEM analysis. Figure 3(b) compares the XRD patterns for PET/15A, PET/30B, and PET/DMIBrC nanocomposites with 3 wt% loading of organosilicate. When the XRD pattern for PET/15A nanocomposite is examined, as shown in Figure 3(b), the PET/15A nanocomposite clearly shows the (001) reflection peak at $2\theta = 2.5°$ which is nearly the same position as that of 15A, indicating that the degree of intercalation of PET chains into the gallery of 15A is very low compared to that of other PET nanocomposites prepared in this study. This may be attributed to two facts: one is that the organic modifier in 15A has no functional group compatible with PET, and the other one is low thermal stability of 15A as revealed in TGA analysis (see Figure 2). As shown in Figure 3(b), the PET/30B nanocomposite shows two reflection peaks at around $2\theta = 2.5$ and $6°$. The broad peak at around $2\theta = 6°$ corresponds to the (001) reflection peak of 30B (see also Figure 3(a)) and the new peak at $2\theta = 2.5°$ arises from the intercalation of PET chains into the gallery of 30B, indicating that the PET/30B nanocomposite has an intercalated structure. Here, it is noted that the (001) reflection peak of 30B ($2\theta = 4.7°$) shifts to higher angle ($2\theta = 6°$) in the PET/30B nanocomposite, indicating that the basal spacing of 30B is decreased in the PET/30B nanocomposite. This is probably because the organic modifier residing in 30B is thermally decomposed during melt-mixing with PET at 280°C. The intercalated structure of PET/15A and PET/30B nanocomposites is also identified
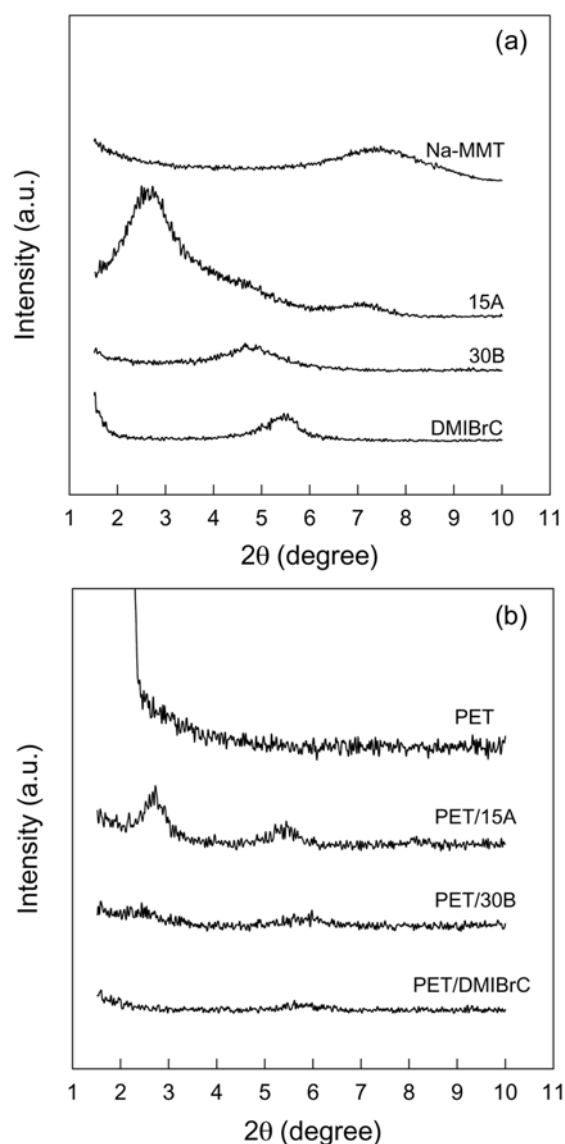

Figure 3. XRD patterns of (a) Na-MMT and organosilicates and (b) PET and PET nanocomposites. In all PET nanocomposites, the amount of organosilicates is fixed at 3 wt%.

by TEM observation. As can be seen in Figures 4(a) and 4(b), the layered structure of organosilicates still remains in
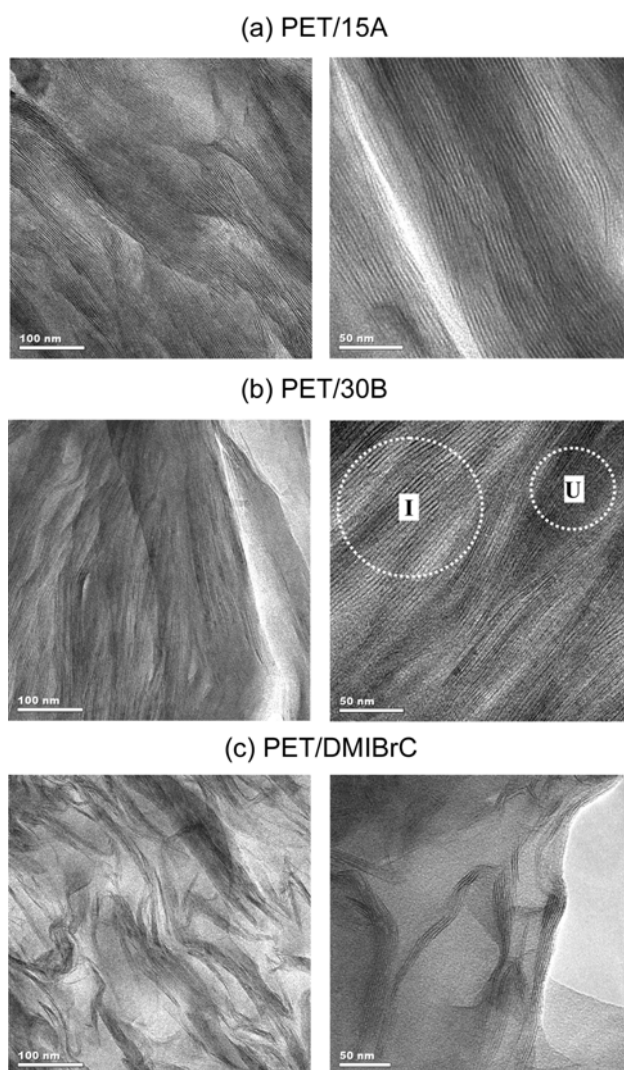
(a) PET/15A

(b) PET/30B

(c) PET/DMIBrC

Figure 4. TEM images of (a) PET/15A, (b) PET/30B, and (c) PET/DMIBrC nanocomposite. Left side images are lower magnification and right ones are higher magnification. In all PET nanocomposites, the amount of organosilicates is fixed at 3 wt%.

the PET/15A and PET/30B nanocomposites, indicating that both PET nanocomposites have intercalated structure. Here, it is interesting to observe that the TEM image for PET/30B nanocomposite clearly shows the coexistence of intercalated (indicated by I) and unintercalated (indicated by U) morphology, as can be seen in Figure 4(b), which is consistent with the results from XRD analysis (see Figure 3(b)). Unlike PET/15A and PET/30B nanocomposites, the XRD pattern for PET/DMIBrC nanocomposite exhibits that the (001) reflection peak of the PET/DMIBrC nanocomposites nearly disappears, as shown in Figure 3(b). However, a closer examination of the XRD pattern for the PET/DMIBrC nanocomposite reveals that a very weak and broad peak at around $2\theta=5.5°$ still remains, indicating that some tactoids of several organosilicates maintaining their layered structure are dis-

persed within the PET matrix. This is clearly evidenced by TEM observation, as shown in Figure 4(c), where the organosilicates are chopped into stacks of several silicate layers and the stacks are well dispersed within the PET matrix. In other words, in PET/DMIBrC nanocomposite, more organosilicates lose their layered structure and are randomly dispersed in the PET matrix as compared to the commercial organoclays, although some organosilicates still maintain their layered structure in chopped stacks.

Tensile Properties. The stress-strain curves of PET and PET nanocomposites are represented in Figure 5, and their tensile properties are summarized in Table II. When tensile properties of PET nanocomposites are compared with those of neat PET, it is realized that the tensile modulus of PET/15A and PET/30B nanocomposites is substantially increased as compared to that of neat PET whereas their tensile strength and elongation at break are lower than neat PET, as shown in Figure 5 and Table II. This trade-off of mechanical properties has been very often reported in many studies.[31-34] Unlike PET/15A and PET/30B nanocomposites, the PET/DMIBrC nanocomposite does not exhibit the trade-off (see also Figure 5 and Table II): The PET/DMIBrC nanocomposite shows an enhanced tensile modulus without sacrifice of the tensile strength and elongation at break. Here, the crystallinity of the samples should be taken into account because tensile properties such as tensile modulus and tensile strength strongly depend on the crystallinity of samples. The crystallinities of the neat PET and PET nanocomposites measured by the XRD method are listed in Table II. The degree of crystallinity of samples is calculated using the relation % crystallinity = $[A_c/(A_c+A_a)] \times 100$, where A_c is the area of crystalline region
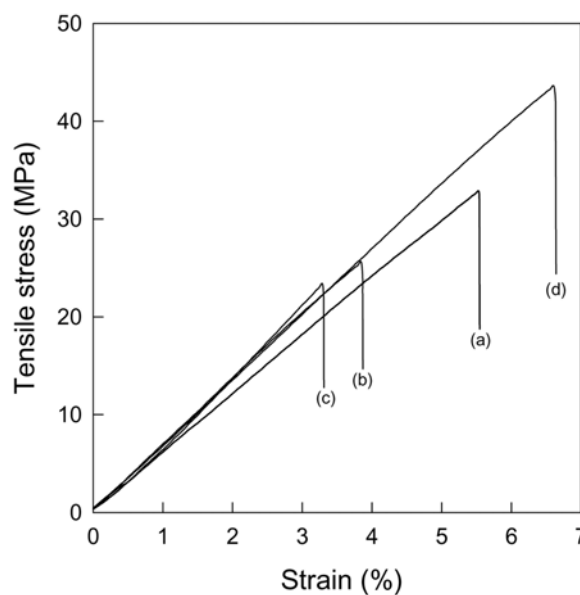

Figure 5. Stress-strain curves for (a) PET, (b) PET/15A, (c) PET/30B, and (d) PET/DMIBrC nanocomposites. In all PET nanocomposites, the amount of organosilicates is fixed at 3 wt%.

Table II. Tensile Properties of the PET and PET Nanocomposites

Samples[a]	Elongation at Break (%)	Strength (MPa)	Modulus (MPa)	Crystallinity (%)
Neat PET	5.5±0.6	33±3	602±16	54
PET/15A	3.8±0.3	25±2	681±15	53
PET/30B	3.3±0.3	25±5	743±12	58
PET/DMIBrC	6.6±0.2	42±2	671±5	57

[a]In all PET nanocomposites, the amount of organosilicates is fixed at 3 wt%.

of samples and A_a is the area of the amorphous region of samples in XRD pattern (see Figure 6). As can be seen in Figure 6 and Table II, the neat PET and PET nanocomposites have nearly equal crystallinity. Therefore, it is reasonable to assume that the effect of crystallinity on tensile properties of PET nanocomposites does not have to be taken into account. This leads us to conclude that enhanced tensile properties of PET/DMIBrC nanocomposite are mainly due to two facts: the degree of exfoliation and/or dispersion of DMIBrC in PET matrix and the degree of affinity between DMIBrC and PET matrix.

The reason why DMIBrC yields more exfoliated PET nanocomposite with better mechanical properties than 15A and 30B may be explained by considering two facts. One is that DMIBrC is thermally more stable than 15A and 30B. Another is that DMIBrC interacts more strongly with PET than 15A and 30B. In other words, the DMIBr synthesized in this study maintains its initial structure during melt-mixing with PET due to its thermal stability (see Figure 2) and is also compatible with PET chains probably due to the specific interaction between the hydroxyl group of DMIBr and the carbonyl group of PET. Therefore, the DMIBr already intercalated in the silicate layers may interact with PET chains during melt-mixing, resulting in partially exfoliated PET nanocomposites. Here, it is noteworthy that the organic modifier in 30B also has a hydroxyl group that can interact with the carbonyl group of PET, but the thermal decomposition of the organic modifier in 30B may become very serious during melt-mixing with PET, as shown in Figure 2, resulting in only the intercalated PET nanocomposite with inferior mechanical properties. In short, the above results lead us to conclude that both the thermal stability of organosilicate and the compatibility between PET and organosilicate play a critical role in preparing exfoliated PET nanocomposite with improved mechanical properties.

Conclusions

This study has demonstrated that the use of new organosilicate (DMIBrC) synthesized in this study yields better exfoliation and/or dispersion of silicate layers in PET than the use of commercial organoclays (15A and 30B). This is because the DMIBrC has better thermal stability and better compatibility with PET than the commercial organoclays. Particularly, the PET/DMIBrC nanocomposite shows higher tensile modulus, higher tensile strength and higher elongation at break as compared with the neat PET, indicating that the PET/DMIBrC nanocomposite overcomes the trade-off behavior between modulus and elongation at break. These results lead us to conclude that both the thermal stability of organosilicate and the compatibility between PET and organosilicate play a critical role in preparing exfoliated PET nanocomposite with superior mechanical properties.

Figure 6. WAXD patterns of (a) PET, (b) PET/15A, (c) PET/30B, and (d) PET/DMIBrC nanocomposites. In all PET nanocomposites, the amount of organosilicates is fixed at 3 wt%.

References

(1) A. Okada, Y. Fukushima, M. Kawasumi, S. Inagaki, A. Usuki, S. Sugiyama, T. Kurauchi, and O. Kamigaito, US Patent 4,739,007 (1988).

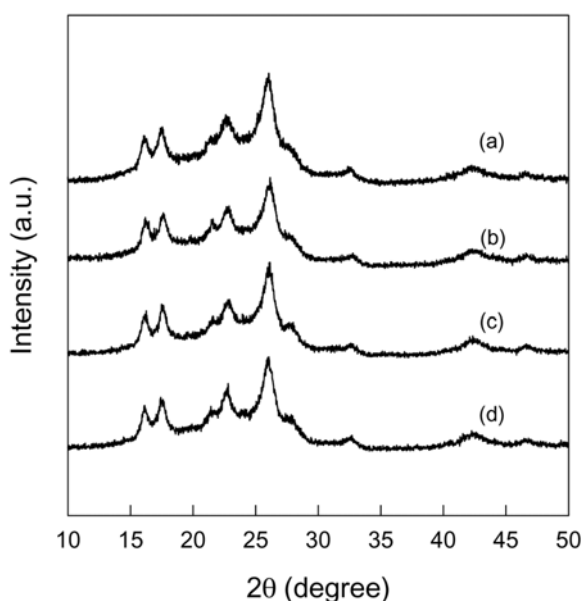(2) A. Usuki, Y. Kojima, M. Kawasumi, A. Okada, Y. Fukushima,

T. Kurauchi, and O. Kamigaito, *J. Mater. Res.*, **8**, 1174 (1993).

(3) A. Usuki, N. Hasegawa, H. Kadoura, and T. Okamoto, *Nano Lett.*, **1**, 271 (2001).

(4) E. P. Giannelis, *Adv. Mater.*, **8**, 29 (1996).

(5) E. P. Giannelis, R. Krishnamoorti, and E. Manias, *Adv. Polym. Sci.*, **138**, 107 (1999).

(6) R. A. Vaia, G. Price, P. N. Ruth, H. T. Nguyen, and J. Lichtenhan, *Appl. Clay Sci.*, **15**, 67 (1999).

(7) H. Shi, T. Lan, and T. J. Pinnavaia, *Chem. Mater.*, **8**, 1584 (1996).

(8) E. P. Giannelis, *Appl. Organomet. Chem.*, **12**, 675 (1995).

(9) R. Xu, E. Manias, A. J. Snyder, and J. Runt, *Macromolecules*, **34**, 337 (2001).

(10) K. Yano, A. Usuki, A. Okada, T. Kurauchi, and O. Kamigaito, *J. Polym. Sci.; Part A: Polym. Chem.*, **31**, 2493 (1993).

(11) R. K. Bharadwaj, *Macromolecules,* **34**, 9189 (2001).

(12) P. B. Messersmith and E. P. Giannelis, *J. Polym. Sci.; Part A: Polym. Chem.*, **33**, 1047 (1995).

(13) J. W. Gilman, *Appl. Clay Sci.*, **15**, 31 (1999).

(14) J. W. Gilman, C. L. Jackson, A. B. Morgan, R. Harris, Jr., E. Manias, E. P. Gianellis, M. Wuthenow, D. Hilton, and S. H. Philips, *Chem. Mater.*, **12**, 1866 (2000).

(15) M. Zanetti, T. Kashiwagi, L. Falqui, and G. Camino, *Chem. Mater.*, **14**, 881 (2002).

(16) M. Zanetti, G. Camino, D. Canavese, A. B. Morgan, F. J. Lamelas, and C. A. Wilkie, *Chem. Mater.*, **14**, 189 (2002).

(17) B. Lepoittevin, M. Devalckenaere, N. Pantoustier, M, Alexandre, D. Kubies, C. Calberg, R. Jerome, and P. Dubois, *Polymer*, **43**, 4017 (2002).

(18) S. W. Kim, W. H. Jo, M. S. Lee, M. B. Ko, and J. Y. Jho, *Polymer*, **42**, 9837 (2001).

(19) K. J. Hwang, J. W. Park, I. Kim, C. S. Ha, and G. H. Kim,

Macromol. Res., **14**, 179 (2006).

(20) B. Lepoittevin, M. Devalckenaere, M. Alexandre, N. Pantoustier, C. Calberg, R. Jerome, and P. Dubois, *Macromolecules*, **35**, 8385 (2002).

(21) W. J. Bae, K. H. Kim, W. H. Jo, and Y. H. Park, *Macromolecules*, **37**, 9850 (2004).

(22) W. J. Bae, K. H. Kim, W. H. Jo, and Y. H. Park, *Polymer*, **46**, 10085 (2005).

(23) J. H. Park, W. N. Kim, H. Kye, S. S. Lee, M. Park, J. Kim, and S. Lim, *Macromol. Res.*, **13**, 367 (2005).

(24) M. T. Defosse, *Mod. Plast.*, **77**, 53 (2000).

(25) J. C. Matayabas, S. R. Turner, Jr., B. J. Sublett, G. W. Connel, and R. B. Barbee, PCT Int Appl WO 29499 (1998).

(26) A. Sanchez-Solis, A. Garcia-Rejon, and O. Manero, *Macromol. Symp.*, **192**, 281 (2003).

(27) A. Pegoretti, J. Kolarik. C. Peroni, and C. Migliaresi, *Polymer*, **45**, 2751 (2004).

(28) W. Xie, Z. Gao, W. P. Pan, D. Hunter, A. Singh, and R. Vaia, *Chem. Mater.*, **13**, 2979 (2001).

(29) J. W. Gilman, W. H. Awad, R. D. Davis, J. Shields, R. H. Harris, Jr., C. Davis, A. B. Morgan, T. E. Sutto, J. Callahan, P. C. Trulove, and H. C. DeLong, *Chem. Mater.*, **14**, 3776 (2002).

(30) C. H. Davis, L. J. Mathias, J. W. Gilman, D. A. Schiraldi, J. R. Shields, P. Trulove, T. E. Sutto, and H. C. Delong, *J. Polym. Sci.; Part B: Polym. Phys.*, **40**, 2661 (2002).

(31) S. T. Lim, J. W. Kim, I. Chin, Y. K. Kwon, and H. J. Choi, *Chem. Mater.*, **14**, 1989 (2002).

(32) S. T. Lim, Y. H. Hyun, H. J. Choi, and M. S. Jhon, *Chem. Mater.*, **14**, 1839 (2002).

(33) K. M. Lee and C. D. Han, *Macromolecules*, **36**, 7165 (2003).

(34) G. X. Chen, H. S. Kim, J. H. Shim, and J. S. Yoon, *Macromolecules*, **38**, 3738 (2005).